

# Path Planning Using Probability Tensor Flows

Francesco A. N. Palmieri <sup>\*†</sup>, Krishna R. Pattipati<sup>†</sup>, Giovanni Fioretti<sup>\*</sup>  
Giovanni Di Gennaro<sup>\*</sup>, Amedeo Buonanno<sup>‡</sup>

<sup>\*</sup>Dipartimento di Ingegneria, Università della Campania “Luigi Vanvitelli”, Aversa (CE), Italy  
{francesco.palmieri, giovanni.digennaro}@unicampania.it,  
giovanni.fioretti@studenti.unicampania.it,

<sup>†</sup>Department of Electrical and Computer Engineering, University of Connecticut, Storrs, CT, USA  
krishna.pattipati@uconn.edu

<sup>‡</sup>ENEA, Energy Technologies Department, Portici (NA), Italy  
amedeo.buonanno@enea.it

**Abstract**—Probability models have been proposed in the literature to account for “intelligent” behavior in many contexts. In this paper, probability propagation is applied to model agent’s motion in potentially complex scenarios that include goals and obstacles. The backward flow provides precious background information to the agent’s behavior, viz., inferences coming from the future determine the agent’s actions. Probability tensors are layered in time in both directions in a manner similar to convolutional neural networks. The discussion is carried out with reference to a set of simulated grids where, despite the apparent task complexity, a solution, if feasible, is always found. The original model proposed by Attias [1] has been extended to include non-absorbing obstacles, multiple goals and multiple agents. The emerging behaviors are very realistic and demonstrate great potentials of the application of this framework to real environments.

**Index Terms**—Bayesian Networks, Factor Graphs, Free Energy, Path Planning

## I. INTRODUCTION

An agent’s intelligent behavior is characterized by goals and environmental constraints in a sea of uncertainties. Probabilistic models provide a very promising framework for manipulating mathematically systems in which only partial knowledge is available. In a real environment, much needs to be learned from experience starting from just a few basic structural rules.

To be able to predict or control agents’ motion in partially structured environments, is a current challenge in a number of applications, ranging from robot planning to self-driving cars to surveillance of critical areas. Many methods have been proposed in the literature. See [2] for a recent comprehensive review. In some of our previous works, we have explored various techniques that include traditional Kalman filter-based approaches [3] [4], models that include social forces [5], polar histograms [6] [7] and Markov models [8].

Work partially supported by POR CAMPANIA FESR 2014/2020, ITS for Logistics, awarded to CNIT (Consorzio Nazionale Interuniversitario per le Telecomunicazioni). Research of Pattipati was supported in part by the U.S. Office of Naval Research and US Naval Research Laboratory under Grants #N00014-18-1-1238, #N00173-16-1-G905 and #HPCM034125HQ, and by a Space Technology Research Institutes grant (number 80NSSC19K1076) from NASAs Space Technology Research Grants Program.

In all cases, motion dynamics have to be properly combined with the environmental constraints in an attempt to capture the agents’ “intelligent” behavior in avoiding obstacles, in interacting with other agents and in attaining specific goals that may be dynamically changing.

There is a growing body of literature that proposes stochastic models based on free-energy principle [9] [10] [11] and KL-learning [12] as general rules of intelligent behavior [13] [14]. There are also interesting connections to causal reasoning [15].

Since the original paper by Attias [1], there has been a growing body of literature in clarifying the connections between Markov Decision Processes (MDPs) and probabilistic approaches [16][17]. The objective function, typically the likelihood function, is combined with the expected reward as explained in a recent review [18].

In this paper, we build on these findings and propose a computational framework in which motion and actions are modeled jointly as probability tensors. Despite the apparent computational complexity of this characterization, motion dynamics can be handled in a manner similar to popular multi-layer neural networks software [19]. Interactions among agents and obstacles in path planning are localized in space, but their consequences are treated globally in a probabilistic model described via forward and backward messages.

Our approach is based on tensor propagation in a *Factor Graph in Reduced normal form (FGrn)* [20]. An FG<sub>rn</sub> is composed of the interconnection of *Single-Input/Single-Output (SISO)* blocks. Tensor messages are propagated bi-directionally and combined using the sum-product algorithm [21]. FG<sub>rn</sub> could be easily augmented to fuse heterogeneous information sources as they become available [20]. In this paper, we limit ourselves to discrete variables, but continuous distributions can be easily handled as in [20][22]. Gaussian messages have been introduced in [23] and used for Kalman filter tracking in [20][22]. More details about factor graphs can be found in the seminal papers [21] and [23]. Further developments on the factor graphs in the reduced normal form are in [20].

In this paper, we explore an application in which states are defined on a 2D finite grid with the additional dimension utilized for actions. This extension allows the distributions on

the map to account for intended motion directions towards one or more goals. Interaction with obstacles are included in the model and the probability flow travels in time in both directions. Forward and backward probability diffusion resembles convolutional operations in multi-layer neural networks.

In this work, the presence of obstacles is modeled as censored/renormalized stochastic conditional distributions, that keep the agent away from obstructions. Therefore, obstacles are not seen as absorbing states [1], but rather as random reflectors that redistribute the probability flow on the map. We will see how the backward flow plays a crucial role in the probabilistic model. Information “coming from the future” may be seen as inverse dynamic modeling, or like a probability field diffused in the environment, or like social interactions. This is a mathematical translation of the fact that intelligent agents generally base their decisions on the impact of projected actions into the future.

Time also plays a crucial role as generally the agents would like to reach their goals in the shortest time possible. We show how minimum time determination is straightforward using the backward flow and how this technique will always be able to find the best feasible paths: the map can be an arbitrarily very complicated maze of regions.

In this paper, we first extend the basic one-agent/one-goal model to include multiple goals: the probabilistic framework allows the inclusion of a distributed set of targets, by the introduction of spread-out probability values at the end of the chain in the backward flow. Furthermore, we extend the model to include multiple agents: each agent is driven by a different probability flow and interacts with the other flows by seeing the other agents as moving obstacles, or as targets. The probability distributions are dynamically updated and the actions for each agent are computed accordingly. We are not aware of similar extensions for such potentially complex scenarios in the literature.

In Section II, we review the basic Bayesian model and its application to path planning. In Section III, we present the state transition model for obstacle avoidance and in Section IV, we discuss the action-control mechanism, that can go from a simple diffusion to the maximum reward policy. The discussion is carried out with reference to various finite grids. Computational complexity and memory requirements are included in Section V and relations to dynamic programming are provided in Section VI. Extensions to multiple goals are in Section VII and the application to more complex multiple-agent tasks is in Section VIII. Section IX discusses conclusions and future developments.

## II. THE BAYESIAN MODEL

Our model for a single agent is based on a sequence of states  $S_t$ ,  $t = 1 : T$ , that are assumed to be fully observable and to belong to a finite space  $\mathcal{S} = \{s^1, \dots, s^{n_S}\}$  and a sequence of “actions”  $A_t$ ,  $t = 1 : T - 1$ , that also belong to a finite space  $\mathcal{A} = \{a^1, \dots, a^{n_A}\}$ . In a general Markov model, both state and actions at time  $t$  are linked to both state and action at time  $t - 1$ . The stochastic model is fully characterized by the pmfs

(probability mass functions)<sup>1</sup>

$$\begin{cases} \pi_{S_1 A_1}(s_1, a_1); \\ p_{S_t A_t | S_{t-1} A_{t-1}}(s_t, a_t | s_{t-1}, a_{t-1}), t = 2 : T - 1; \\ p_{S_T | S_{T-1} A_{T-1}}(s_T | s_{T-1}, a_{T-1}). \end{cases} \quad (1)$$

To be more specific about mutual connections, let us rewrite the general pmf as

$$\begin{aligned} & p_{S_t A_t | S_{t-1} A_{t-1}}(s_t, a_t | s_{t-1}, a_{t-1}) \\ &= \frac{p_{S_t A_t S_{t-1} A_{t-1}}(s_t, a_t, s_{t-1}, a_{t-1})}{p_{S_{t-1} A_{t-1}}(s_{t-1}, a_{t-1})} \\ &= \frac{p_{A_t | S_t S_{t-1} A_{t-1}}(a_t | s_t, s_{t-1}, a_{t-1}) p_{S_t | S_{t-1} A_{t-1}}(s_t, s_{t-1}, a_{t-1})}{p_{S_{t-1} A_{t-1}}(s_{t-1}, a_{t-1})} \\ &= p_{A_t | S_t S_{t-1} A_{t-1}}(a_t | s_t, s_{t-1}, a_{t-1}) \\ & \quad \cdot p_{S_t | S_{t-1} A_{t-1}}(s_t | s_{t-1}, a_{t-1}). \end{aligned} \quad (2)$$

Now, if we drop the conditional dependence of  $A_t$  on  $S_{t-1}$ , we have the factorized model

$$\begin{aligned} & p_{S_t A_t | S_{t-1} A_{t-1}}(s_t, a_t | s_{t-1}, a_{t-1}) \\ &= p_{A_t | S_t A_{t-1}}(a_t | s_t, a_{t-1}) p_{S_t | S_{t-1} A_{t-1}}(s_t | s_{t-1}, a_{t-1}), \end{aligned} \quad (3)$$

depicted in Figure 1.

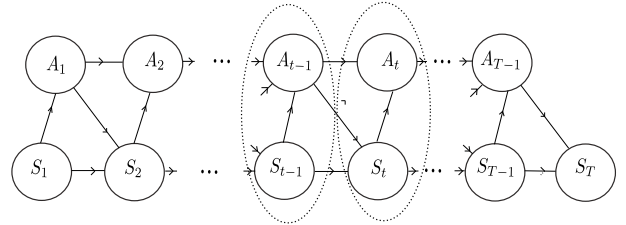


Fig. 1: State-Action Markov Model as a Bayesian graph

Note that the factor  $p_{S_t | S_{t-1} A_{t-1}}(s_t | s_{t-1}, a_{t-1})$  represents the physical system (plant), i.e., how the state changes according to the previous state and action. The factor  $p_{A_t | S_t A_{t-1}}(a_t | s_t, a_{t-1})$  is the rule (controller), in general stochastic, with which new actions are generated as a consequence of the current state and the previous action. This is a standard stochastic model used in MDPs (Markov Decision Processes) [24][25], where  $p_{A_t | S_t A_{t-1}}$ ,  $i = 1, \dots, T - 1$ , is also usually expressed as a *policy*  $\pi$ . Action policy will be introduced in a following discussion also because in our formulation,  $(A_t, S_t)$  will be treated together by the control action.

Recognizing the cliques in Figure 1, we can reduce the system to the Markov chain depicted in the middle of Figure 2 as a Factor Graph. Belief propagation can be performed on the graph with states and actions at each time  $t$  considered jointly. Therefore, all forward ( $f$ ) and backward ( $b$ ) messages are defined on the  $n_S \times n_A$  dimensional space  $\mathcal{X} \times \mathcal{A}$ .

Using the shortened notation, forward and backward mes-

<sup>1</sup>We use upper case letters for random variables and lower case letters for their values.

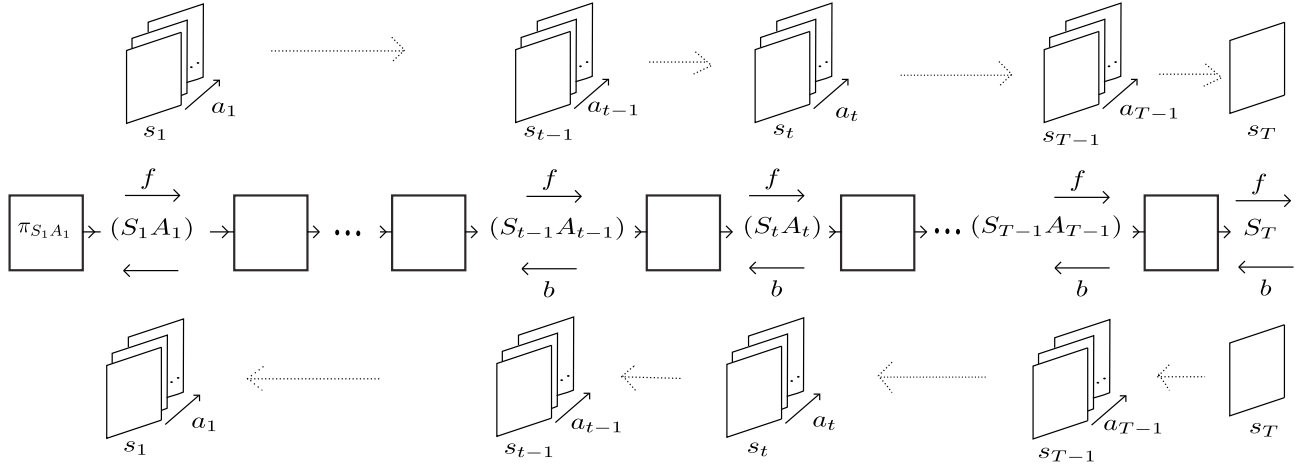


Fig. 2: State-Action Markov Model as a Factor Graph with forward (top) and backward (bottom) tensor flows.

sages are composed using the sum rule [21][20]

$$\begin{aligned}
 f(s_1, a_1) &= \pi(s_1, a_1); \\
 f(s_t, a_t) &= \\
 &\sum_{a_{t-1}} p(a_t | s_t, a_{t-1}) \sum_{s_{t-1}} p(s_t | s_{t-1}, a_{t-1}) f(s_{t-1}, a_{t-1}) \\
 &\quad t = 2 : T - 1; \\
 f(s_T) &= \sum_{a_{T-1}} \sum_{s_{T-1}} p(s_T | s_{T-1}, a_{T-1}) f(s_{T-1}, a_{T-1}); \\
 b(s_{T-1}, a_{T-1}) &\propto \sum_{s_T} p(s_T | s_{T-1}, a_{T-1}) b(s_T); \\
 b(s_{t-1}, a_{t-1}) &\propto \\
 &\sum_{a_t} p(a_t | s_t, a_{t-1}) \sum_{s_t} p(s_t | s_{t-1}, a_{t-1}) b(s_t, a_t) \\
 &\quad t = T - 1 : 2
 \end{aligned} \tag{4}$$

Posterior distributions, are obtained with the product rule [21][20]

$$\bar{p}(s_t, a_t) \propto b(s_t, a_t) f(s_t, a_t). \tag{5}$$

Note that the forward messages, are normalized distributions, if  $\pi(s_1, a_1)$  is normalized, while the backward messages and the posteriors are only proportional to their respective pmfs. In belief propagation, messages and posteriors can be kept unnormalized even if it is preferable to normalize them for numerical stability [21][20]. The reader not too familiar with probability propagation should be aware that these rules are rigorous translations of Bayes' theorem and marginalization.

Our discussion will be carried out with reference to a 2D scenario in which the states are defined on an  $N \times M$  finite grid

$$S_t = (X_t, Y_t), \quad X_t \in \{1, \dots, M\}; \quad Y_t \in \{1, \dots, N\}, \tag{6}$$

$n_S = N \cdot M$ . In our examples, there are nine possible actions:

$$\begin{aligned}
 \mathcal{A} = \{a^1, \dots, a^9\} = \{ &\text{still, up, up-right, right,} \\
 &\text{down-right, down, down-left, left, up-left} \}
 \end{aligned} \tag{7}$$

Hence, all the distributions are tensors in which the first two dimensions are the coordinates on the grid and the third dimension is the action (Figure 2, top and bottom).

### III. THE STATE-TRANSITION MODEL

The probability function  $p_{S_t | S_{t-1}, A_{t-1}}(s_t | s_{t-1}, a_{t-1})$  describes the system state transition at time  $t$  as a consequence of the previous state and action. In our 2D implementation, in the absence of obstacles, the stochastic motion is described in Figure 3, where the distribution is limited to one step away from the previous position and it is mostly concentrated in the direction of the intended motion. The probabilities shown in the figure are only a possible choice. The distribution could be sharper to reflect more determined action in each direction, or be smoother for an agent that moves more randomly. Furthermore, larger masks could be easily defined to model agents that may move more than one step at a time.

$i-1$	$\frac{1}{16}$	$\frac{1}{16}$	$\frac{1}{16}$	$\frac{1}{6}$	$\frac{1}{3}$	$\frac{1}{6}$	$\frac{1}{18}$	$\frac{1}{6}$	$\frac{1}{3}$
$i$	$\frac{1}{16}$	$\frac{1}{2}$	$\frac{1}{16}$	$\frac{1}{18}$	$\frac{1}{18}$	$\frac{1}{18}$	$\frac{1}{18}$	$\frac{1}{18}$	$\frac{1}{6}$
$i+1$	$\frac{1}{16}$	$\frac{1}{16}$	$\frac{1}{16}$	$\frac{1}{18}$	$\frac{1}{18}$	$\frac{1}{18}$	$\frac{1}{18}$	$\frac{1}{18}$	$\frac{1}{18}$
$i-1$	$\frac{1}{18}$	$\frac{1}{18}$	$\frac{1}{6}$	$\frac{1}{18}$	$\frac{1}{18}$	$\frac{1}{18}$	$\frac{1}{18}$	$\frac{1}{18}$	$\frac{1}{18}$
$i$	$\frac{1}{18}$	$\frac{1}{18}$	$\frac{1}{3}$	$\frac{1}{18}$	$\frac{1}{18}$	$\frac{1}{6}$	$\frac{1}{18}$	$\frac{1}{18}$	$\frac{1}{18}$
$i+1$	$\frac{1}{18}$	$\frac{1}{18}$	$\frac{1}{6}$	$\frac{1}{18}$	$\frac{1}{6}$	$\frac{1}{3}$	$\frac{1}{6}$	$\frac{1}{3}$	$\frac{1}{6}$
$i-1$	$\frac{1}{18}$	$\frac{1}{18}$	$\frac{1}{18}$	$\frac{1}{6}$	$\frac{1}{18}$	$\frac{1}{18}$	$\frac{1}{3}$	$\frac{1}{6}$	$\frac{1}{18}$
$i$	$\frac{1}{6}$	$\frac{1}{18}$	$\frac{1}{18}$	$\frac{1}{3}$	$\frac{1}{18}$	$\frac{1}{18}$	$\frac{1}{6}$	$\frac{1}{18}$	$\frac{1}{18}$
$i+1$	$\frac{1}{3}$	$\frac{1}{6}$	$\frac{1}{18}$	$\frac{1}{6}$	$\frac{1}{18}$	$\frac{1}{18}$	$\frac{1}{18}$	$\frac{1}{18}$	$\frac{1}{18}$
	$j-1$	$j$	$j+1$	$j-1$	$j$	$j+1$	$j-1$	$j$	$j+1$

Fig. 3: State transition distributions for  $(X_t, Y_t)$  conditioned on the previous state being in  $(x_{t-1}, y_{t-1}) = (i, j)$  and  $a_{t-1} = \text{still, up, up-right, right, down-right, down, down-left, left, up-left}$  (in lexicographic order).

The inclusion of obstacles and boundaries (obstructions) in the definition of  $p_{S_t | S_{t-1}, A_{t-1}}(s_t | s_{t-1}, a_{t-1})$  is crucial to obstacle avoidance and best path selection strategies. Boundaries and obstacles are defined on the state grid with an  $N \cdot M$  binary mask  $W = [w_{ij}]$ , with  $w_{ij} = 1$ , if there is an obstacle in  $(i, j)$  and  $w_{ij} = 0$  for free locations.

In our implementation, we have assumed that the obstacles

are avoided, with a mechanism that censors and renormalizes the transition distribution as shown in the example of Figure 4: when the transition distribution overlaps an obstacle, the overlapping probabilities are set to zero and the others are renormalized. This means that the agent is reflected (discouraged) by the obstacles and is projected onto the non-overlapping pixels with the same probabilities, but renormalized.

Figure 6 shows the localized operations in the forward and in the backward flow. They resemble a layer in a convolutional multi-layer network. The difference here is that the convolutional filters are not space-invariant as they depend on the map. Furthermore, the coefficients are probabilities and there are possible normalizations. A direct correspondence to a multi-layer neural network is an intriguing problem and it is currently under investigation.

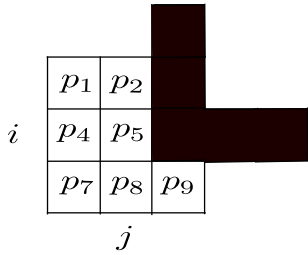


Fig. 4: Example of state transition renormalization in the presence of an obstruction. We are at time  $(t - 1)$  and  $p_1, \dots, p_9$  would be the probabilities  $p((x_t, y_t)|(x_{t-1}, y_{t-1}) = (i, j), a_{t-1} = \bar{a})$  for a specific action  $\bar{a}$  (one of the masks in Figure 3) if we had no obstruction. Since pixels  $(i - 1, j + 1)$  and  $(i, j + 1)$  are obstructed,  $p((x_t, y_t)|(x_{t-1}, y_{t-1}) = (i, j), a_{t-1} = \bar{a})$  is redefined with  $p_3, p_6 \leftarrow 0$  and  $p_i \leftarrow \frac{p_i}{1 - p_3 - p_6}$ ,  $i = 1, 2, 4, 5, 7, 8, 9$ .



Fig. 5: A  $15 \times 15$  grid with Start (S), Goal (G), obstacles and boundaries.

#### IV. THE CONTROL MODULE

Action generation at time  $t$  is described by the pmf  $p(a_t|s_t, a_{t-1})$  that models the new action as a consequence of previous action  $a_{t-1}$  and current state  $s_t$ . This is the crucial control part of the agent’s behavior that, in a complete scenario, should depend also on projected inference into the future and the goal via a certain policy  $\pi$  as in MDP [24][25][16].

##### A. Pure diffusion

We look first at a simplified scenario in which the agent moves in a pure diffusion mode driven by the pmf  $p(a_t|a_{t-1})$ ,

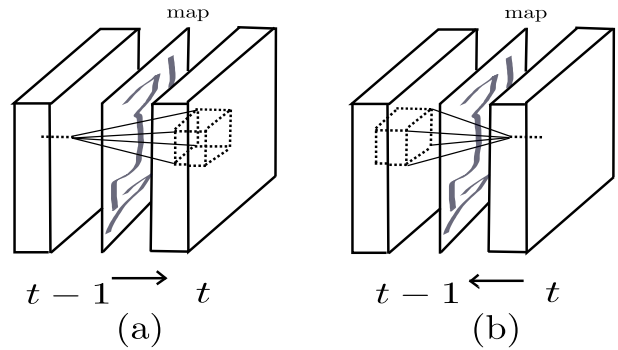


Fig. 6: Diffusion in the forward (a) and in the backward flow (b).

independently from the state and keeping only possibly a memory on the previous action  $a_{t-1}$ . This action memory allows the modeling of motion stiffness, i.e. a tendency of the agent to maintain its course, or in general to maneuver according to a Markov process (with no relation to the state). Since we have  $n_A$  possible actions (in our example  $n_A = 9$ ),  $p(a_t|a_{t-1})$  is described by an  $n_A \times n_A$  row-stochastic matrix  $P_A$ .

In this first analysis of our model, we assume that initial (start) and the final (goal) state are fixed (Attias’ model [1]) (in Bayesian networks’ terms we say that the states  $S_1 = \bar{s}$  and  $S_T = \bar{g}$  have been *instantiated*). This corresponds to messages at the beginning and at the end of the chain

$$f_{S_1 A_1}(s_1, a_1) = \delta(s - \bar{s})\pi_{A_1}(a_1); \quad b_{S_T}(s_t) = \delta(s - \bar{g}), \quad (8)$$

where  $\pi_{A_1}(a_1)$  is the initial action distribution. If we set a deterministic initial action  $a_1 = \bar{a}$ , we have  $\pi_{A_1}(a_1) = \delta(a_1 - \bar{a})$ , where  $\delta(x) = 1$ , for  $x = 0$  and zero else.

Figure 5 shows a  $15 \times 15$  grid, in which an agent from a starting point S, has to find his way through a set of obstacles to reach the goal G. Boundaries are considered obstacles and handled with the reflection mechanism explained in Figure 4. The time horizon is  $T = 23$ . Initial action distribution is set to uniform and the action transition matrix  $P_A$  is uniform (1/9 in all entries).

Figure 7 shows the results of a pure diffusion on the grid of Figure 5. The three rows show forward, backward and posterior distributions at time steps  $t = 4, 13, 20$ . Recall that each distribution is three-dimensional and action is in the third dimension. State probabilities (marginalized over actions), are shown proportional to the pixel intensity and the action probabilities are shown as arrows in each pixel: each arrow points in the direction of maximum action probability. Furthermore pixels with a dot correspond to maximum action probability on “still”. Crosses denote uniform action distributions.

Note how the forward distribution is a pure diffusion with no preferred direction. Backward distributions are instead “inverse diffusion” starting from the goal at time  $T$  and working their way back into the past. Posterior distributions, that are the normalized product of forward and backward messages, show the most likely regions and directions in time compatible with the agent reaching the goal at time  $T$ . The crucial aspect of this analysis is the presence of the action dimension that gives

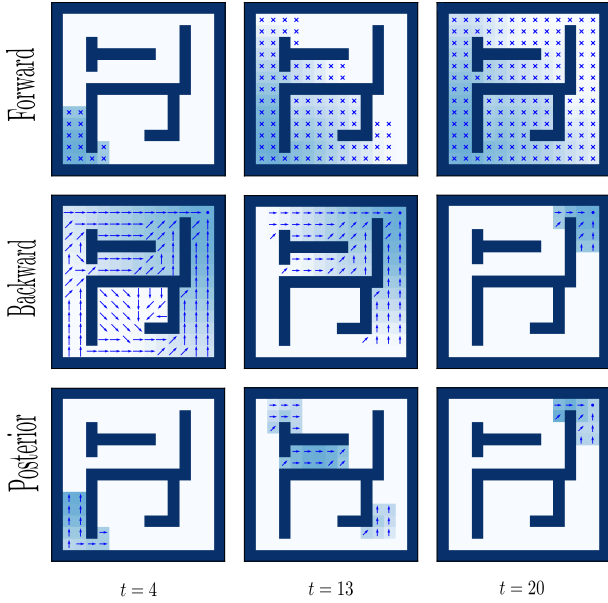


Fig. 7: Forward, backward and posterior distributions at time steps  $t = 4, 13, 20$ , in a pure diffusion mode. State probabilities, marginalized over actions, are shown at different locations in shades of blue. Action probabilities are shown on each location as arrows pointing in the direction of maximum probability. A dot denotes that the maximum probability is for “still”. Crosses denote uniform action distributions. The time horizon is  $T = 23$  (not minimum).

direction to the motion. The distribution on position only on the grid, would not give us complete information on how the probability flow progresses.

Note how the backward flow resembles a vector field suggesting intriguing relations between this stochastic model and traditional field theory. It is as if the backward flow was leaving tracks on the grid (“a yellow brick road”) that must be followed to reach the goal in the set time. We have verified that no matter how complicated the maze is, if a feasible path exists, the combination of forward and backward diffusion always concentrates the probability mass in the appropriate regions of the space, where the agent should be located in time to reach the goal.

The main limitation of the pure diffusion model, is that the time it takes to reach the goal has to be pre-determined [1][16]. If  $T$  is too small, there exist no regions where the agent can be found that are compatible with the agent reaching the goal: the posterior probability is zero because forward and backward flows are always such that one of them is zero. If  $T$  is too large, the agent can span the space with more freedom and there are many (sub-optimal) ways of reaching the goal.

Figure 8 shows the posterior distribution at three time steps, when the time horizon has been set to exactly the minimum  $T = T_{min} = 18$ . There are only small regions where the agent may be found at any given time. Only those locations are compatible for the agent to reach the target with a minimum length path. This is to be compared with the posterior in Figure 7 where the time horizon has been set to a non-minimum value ( $T = 23$ ), for which there are wide regions where the agent

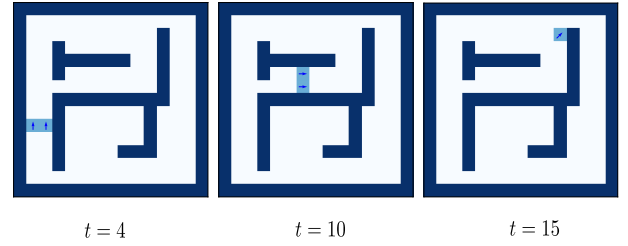


Fig. 8: Posterior distribution for  $T = T_{min} = 18$ ,  $t = 4, 10, 15$

may be located at any given time.

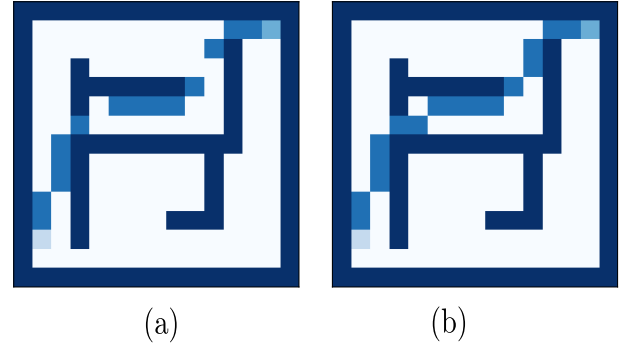


Fig. 9: (a) The set of maximum posterior points for  $T = 23 > T_{min}$  (note the disconnected path); (b) The set of maximum posterior points for  $T = T_{min} = 18$ .

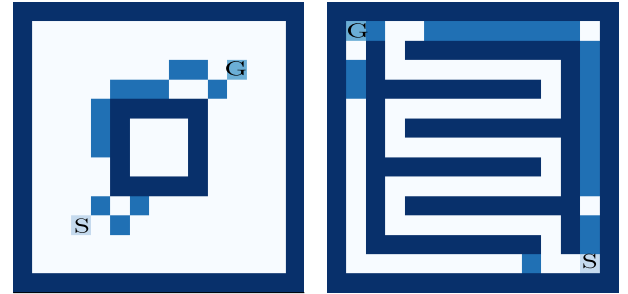


Fig. 10: (a) The set of maximum posterior points for  $T = T_{min}$  on two grids where the path results disconnected.

1) *Path determination*: Maximization of the total likelihood would suggest that, to determine the path to destination, we just have to compute the points of maxima in the posterior distribution. Unfortunately, this unconstrained solution may provides disconnected paths as shown in Figure 9(a). When a non-minimum time horizon is chosen, the agent has more time to reach the goal: it can be more freely located in larger areas where the posterior distribution may take various configurations. We have also verified that using the means, rather than the maxima, would not change much. Figure 9(b) shows the results of choosing minimum time. In this case, the more constrained posterior support produces a connected path. Unfortunately, even with minimum time, we are not guaranteed that the path with the maxima points is connected. Figure 10 shows two more examples where, even if the time horizon is set to the minimum value, we obtain disconnected

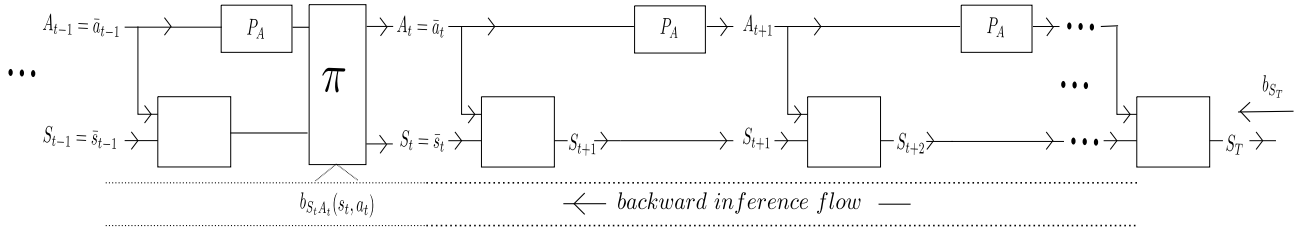


Fig. 11: Block diagram of the plant-controller system at time  $t$ . The backward message at  $T$  is  $b_{S_T}(s_T) = \delta(s_T - \bar{s}_T)$ .

paths. This effect seems to be more pronounced when we have multiple minima.

2) *Minimum time determination*: Even if a pure diffusion model (no action control) cannot guarantee connected paths, it may be useful to compute minimum time. This can save time in the computations and gives us a frame of reference for the scenario with control included that follows. The minimum time can be computed through probability diffusion in a straightforward way using the backward flow: *run the backward flow until at the start position there is a non-zero probability*. This is another nice feature of using probability propagation.

### B. Introducing state-dependent actions

Path determination in general should not depend on the minimum time determination. More specifically, it should be determined using an algorithm that fixes the state and the action at every time step and then takes an informed decision to evolve to the next step. This is what the state-dependent action discussed in this section does.

The probabilistic model shown above demonstrates that the interaction between the forward and the backward information flow can provide a framework for solving an apparently very complicated problem. The great feature of this model, is that the backward flow, that corresponds to running the agents' dynamics backward in time, can provide a nice track for guided behaviour. Figure 11 is a block diagram of the system at time  $t$ , that it is now a hybrid architecture that mixes probabilistic inferences with decisions. The system has to generate a single path with a sequence of specific instances  $\{\bar{s}_t, \bar{a}_t\}_{t=1}^T$  with actions and states now generated using also backward information coming from the future. The agent is driven by an algorithm that uses goal diffusion "rolled" back from the future in a way similar to the case of pure diffusion.

Figure 11 shows the situation at a generic time  $t$ , where at previous time steps decisions on states and actions have been taken. At time  $t - 1$ , we have an instance  $(S_{t-1}, A_{t-1}) = (\bar{s}_{t-1}, \bar{a}_{t-1})$  and the controller follows a policy  $\pi$  to set  $(S_t, A_t) = (\bar{s}_t, \bar{a}_t)$ . Note that backward information from the future is based on pure diffusion: no specific control action is projected into the future. Nevertheless the backward distributions provide guidance to choose appropriate state and actions towards regions of larger probabilities. Note also that *the action policy treats  $(A_t, S_t)$  jointly*.

The following algorithm follows a greedy strategy and finds a connected path.

*G-algorithm Outline*:

(a) Initialize state (goal) at time  $t = T$  with  $b_{S_T}(s_t) = \delta(s - \bar{g})$ ;

- (b) Compute the complete backward flow using the last two equations in (4) from  $t = T$  to  $t = 2$ ;
- (c) Initialize the state and action (start) at time  $t = 1$  with  $f_{S_1 A_1}(s_1, a_1) = \delta(s_1 - \bar{s}, a_1 - \bar{a})$ ;
- (d) Set  $t \leftarrow t + 1$  and compute the forward distribution  $f_{S_t A_t}(s_t, a_t)$  using the second equation in (4);
- (e) Compute the posterior distribution:
 
$$p_{S_t A_t}(s_t, a_t) \propto f_{S_t A_t}(s_t, a_t) b_{S_t A_t}(s_t, a_t);$$
- (f) Set  $(S_t, A_t) = (\bar{s}_t, \bar{a}_t) = \operatorname{argmax} p_{S_t A_t}(s_t, a_t)$ ;
- (g) Replace forward distribution as:
 
$$f_{S_t A_t}(s_t, a_t) = \delta(s_t = \bar{s}_t, a_t = \bar{a}_t)$$
- (h) Back to (d) for the next time step.

The algorithm essentially maximizes the likelihood in a greedy fashion. The solution is reached much like in the Viterbi algorithm (poor man's Viterbi) in a large-dimensional space. Therefore, if the time horizon is set to minimum time, the solution is optimal.

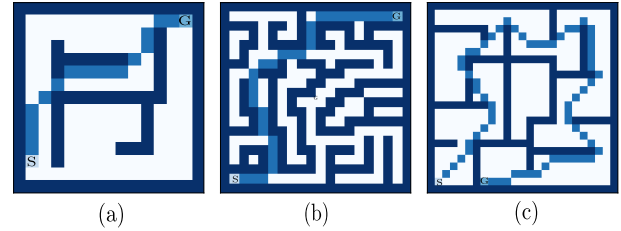


Fig. 12: Path found by the G-algorithm for: (a) the grid of Figure 5; (b) (c) two more complex grids.

Figure 12(a) shows the path resulting from the above G-algorithm for the grid of Figure 5. We have verified that, no matter how complicated the maze is, the procedure always finds a connected path to the destination if a feasible time  $T$  has been set. Figure 12(b) and (c) show the paths found for two more grids  $20 \times 20$  and  $25 \times 25$ , respectively. For the time horizon, we have used the minimum time for all ( $T_{min} = 18, 32, 64$  respectively). When the time is not minimal, the path may oscillate around its final destination, but there is always a non-null probability on the goal.

1) *Algorithm variations*: In the G-algorithm, a number of small variations may be adopted for more robust implementations, or for different applications:

1. When the algorithm runs on non-minimum time, a control to stop the evolution can be added when the agent steps on the goal. This would avoid that the agent keeps wandering around and that the path increases its length.

2. During evolution, at specific time  $t$  and at locations around the current agent's position, it may happen that the

posterior is null. This may be caused by an insufficient time horizon  $T$ , or because there is no feasible solution (forward and backward flows do not meet). In such cases, for a single agent, the algorithm will give no answer. As we will see in the following, when there are multiple agents, i.e. the map is dynamically changing, we may adopt different strategies. For example, a random action could be taken according to the forward distribution, or simply wait for a solution to become feasible.

3. The algorithm can be used in a generative mode to produce a collection of paths. In this case, randomized actions could be taken following the same distributions available in the probability flow. For example, at time  $t$ , the next action can be sampled from the posterior  $p_{S_t A_t}(s_t, a_t) \propto f_{S_t A_t}(s_t, a_t) b_{S_t A_t}(s_t, a_t)$  as shown in Figure 13. When the time horizon is set to the minimum value (top row), the agent’s different realizations are all best paths. Conversely, when  $T$  exceeds the minimum time (bottom row), the agent has much more freedom to wander around and may take paths in different regions.

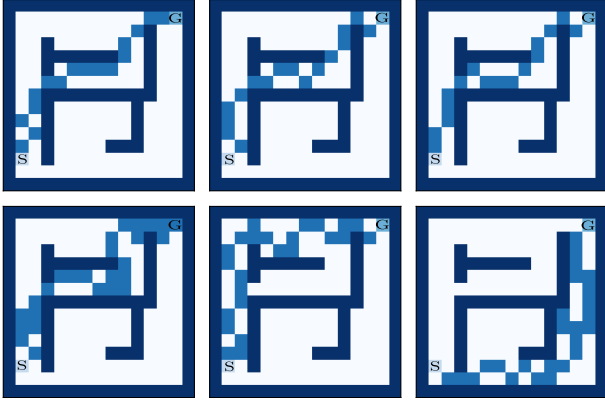


Fig. 13: A collection of random paths following the same model (top row:  $T = T_{min} = 18$ ; bottom row:  $T = 30$ ).

### C. Steady state

Forward and backward flows evolve according to the rules of probability propagation, explained in Section II and shown in Figure 7 for an example. Even if they are time-dependent, one may wonder whether the probability flow, more specifically the backward flow, after a sufficient number of time steps, may reach a steady-state configuration. If such a convergence were verified, a unique configuration would allow simple memorization of just one tensor and not the whole time-dependent flow. Unfortunately, the presence of obstacles and the reflection mechanism causes the flows to oscillate in time and a steady-state configuration can be reached only in free areas. We have experimented using the backward tensor (propagated back) at time  $t = 1$  throughout the whole time horizon. We have found that the agent may fail to reach his goal, because it may undergo oscillatory behavior in the vicinity of obstacles.

## V. COMPLEXITY AND MEMORY

Tensor manipulation can become computationally heavy when we have to deal with large grids, for example,

when the scene is modeled at high resolution. Complete memorization of the probability flow (forward, backward and posterior) for the overall time horizon  $T$ , requires  $\#real\ value\ memory\ cells = 3NMn_A T$ . The convolution-like computation of at every time step requires  $\#operations = n_A^2 NM$  both for forward and backward flow. Posterior computation requires  $n_A NM$  multiplications at every time step. Overall, the computational complexity can be estimated to be in the order of  $O(n_A^2 NMT)$ . To have an idea, a  $100 \times 100$  grid with  $n_a = 9$  with a time horizon of 100, requires approximately 27M locations and a total number of operations in the order of 81M (no graphics). To have a frame of reference, on a laptop with CPU i7-9750H for a grid  $25 \times 25$  and  $T = 64$ , our typical simulation runs in about 200 seconds, graphics included.

## VI. RELATION TO MDP AND DYNAMIC PROGRAMMING

There is clearly a connection between the Bayesian approach to path planning discussed here and dynamic programming that projects actions into the future to adopt control policies. In dynamic programming, there is a reward mechanism connected to states and actions at every time step. In the probabilistic approach presented in this paper, even if reward nodes could be included in the graph (influence diagrams [26]), they are left out for now and the only connection to the objectives are in the goal position and in the messages propagated back from the final time  $T$ . By definition of Bayesian networks, maximization of posterior probabilities corresponds to the maximization of the total likelihood

$$L = \pi_{S_1 A_1}(s_1, a_1) \sum_{t=2}^{T-1} p_{S_t A_t | S_{t-1} A_{t-1}}(s_t, a_t | s_{t-1}, a_{t-1}) p_{S_T | S_{T-1} A_{T-1}}(s_T | s_{T-1}, a_{T-1}). \quad (9)$$

A comparison with finite time MDP with infinite time horizon, has been established by Toussaint, [16] that considers a mixture of models with a finite random  $T$ , distributed according to a discount-like prior  $P(T) = \gamma^T(1 - \gamma)$ . By using a fixed reward  $r = 1$  at every time step, he establishes the equivalence of the likelihood maximization to the expected total reward. Many are the variations available for implementing value iteration in the MDPs. For example, in path planning, details on how to introduce obstacles may also vary. However, Attias’ probability propagation idea on fixed time [1], on which we have built most of our experiments, seems to be much more appealing for visualizing the directional flow: once established, the minimum time  $T$  necessary to reach the goal, as we have suggested above, with our renormalization model for obstacle avoidance, the agent is guaranteed to reach his objective in minimum time.

## VII. MULTIPLE GOALS

This probabilistic framework allows great flexibility in modeling the agent’s motion. For example, there may be more than one target. Distributed goals can be introduced, by injecting at the end of the chain a backward message distributed over multiple locations. Figure 14 shows the results of simulations with an agent that has to reach more than one goal. Various scenarios can be considered:

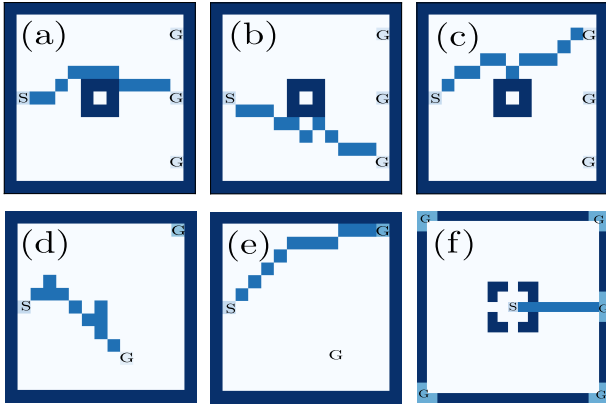


Fig. 14: Paths obtained with multiple goals. In (a-c) there are three goals with the same backward probability and at the same distance from the start: the agents randomly chooses one of them. In (d) the two goals have backward probability 0.2 and 0.8, for the closer and the farthest respectively. The agents essentially ignores the farthest goal. In (e) we have the same situation of (d), but the backward probabilities are pushed to .0001 and .9999: here the agent does have enough “attraction” from the farthest goal and sometimes it goes there. Plot (f) is a grid with many doors as goals. Since here the backward probabilities are uniform, the agent goes toward the closest door at the closest point.

1. The time horizon  $T$  is set to the minimum value for the farthest goal, and the backward distribution at  $T$  is uniform on all the goals. In this case, the greedy algorithm  $G$  always tends to reach the goal at the minimum distance, because the likelihood is maximized. If the actions are randomized, all goals may be reached, but in the various realizations we have lower occurrence for the farthest ones. Figures 14(a-c) show three occurrences for one agent and three goals in which all the goals are at the same distance and  $T = T_{min} = 13$ .

2. For an agent to reach the farthest goal more often, backward probabilities may be controlled. For example, in Figure 14(d), we have set probabilities 0.2 and 0.8 on the two goals. However, they are not sufficient to direct the agent toward the farthest goal often enough: the picture shows a path to the closest path, but in multiple trials we have never seen the farthest goal reached. In Figure 14(e) the farthest goal has been assigned a probability of 0.9999 and the closest 0.0001. The agent reaches the farthest goal more often and the picture shows such a captured realization. In the field theory analogy, the attraction force associated to the backward flow, for the farthest source, has to equalize, or overcome, the other.

3. Multiple goals may be distributed on arbitrary locations in the grid to model the presence of doors or target areas. Figure 14(f) shows a grid with many doors. In that case, the probabilities injected at the end are uniform and the agent tends to go towards the closest door. Unbalanced backward probabilities would produce other paths.

Variation on this scenario, both on maps and goal distributions, have been included in our experiments and are not reported here for brevity.

## VIII. MULTIPLE AGENTS

We have started to use this probabilistic framework to model much more complicated situations, such as those arising when there are multiple agents that have to reach different goals. Figure 15 shows a diagram with  $L$  agents that keep their probability flow updated according to both static and dynamically-changing map and goals. The agents are scheduled to act in a sequence (that can also be randomly permuted), and have their current state visible to the others. This is our first cut to approach parallel behavior, by assuming that each agents acts independently from the others, but sees the others just as obstacles, and/or as goals. Clearly, the map and/or the goals for each agent change at every time step and the whole probability flow has to be recomputed dynamically. We have run many simulations with multiple agents and the emerging behaviors are amazingly close to what is observed on real scenarios!

Figure 16 shows a grid where there are two agents that are trying to reach their respective goals on a map with a narrow passage that does not allow simultaneous crossing. What happens running the two probability flows in parallel, is that when one of the two agents “sees” that the path becomes obstructed (no feasible solution exists at that time step to reach the goal), the agent “waits” until a feasible solution becomes available. As pointed out in one of the above sections, when a solution is not available, the agent can adopt various strategies that go from staying still, or move randomly (in our case the agents wait). Since the grid is continuously changing and the agents’ actions are scheduled in a sequence, the probability flows will possibly change favorably and the agent will be guided in the right direction.

Agents could also be “looking for each other” by simply setting each agent’s position as the goal for one or more other agents. The results of these simulations will be reported elsewhere.

In Figure 17, there are five agents, each trying to reach its goal. Only nine frames are shown. The limitations of static images does not show the full potential of the model that causes the agents to avoid each other, to wait if necessary, to take different paths, etc. (see caption). Animated plots will be made available on our website.

## IX. CONCLUSIONS AND FUTURE WORK

The probabilistic framework to model motion in complex scenarios is very promising because it accounts for “intelligent” behaviors. We have shown how tensor messages can be used to solve apparently very complex path planning problems. The forward and the backward flows, that are derived from the Bayesian formulation, are available to the agent that has to undertake the proper actions to reach his final goal. It clearly demonstrates the crucial role played by the backward flow, that being essentially the system running backward in time, provides guidance into the future. The backward flow resembles a vector field and the consequences of this findings are intriguing also in the context of free-energy models.

In this paper, we have first extended the single-agent framework to distributed goals, where, in realistic settings, the model can easily include doors, benches, counters, food sources, etc.



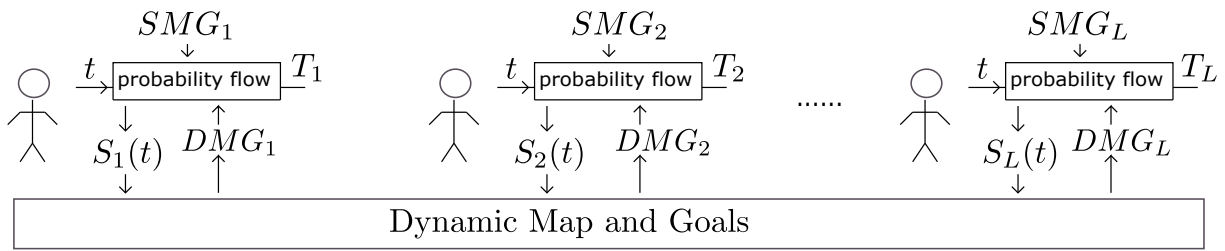


Fig. 15: Interacting agents that keep their probability flow updated according to their Static Map and Goals (SMG) and their Dynamic Map and Goals (DMG). The agents, scheduled in sequence, have knowledge of the current state of the others, that is translated in dynamically changing individual map and goals.

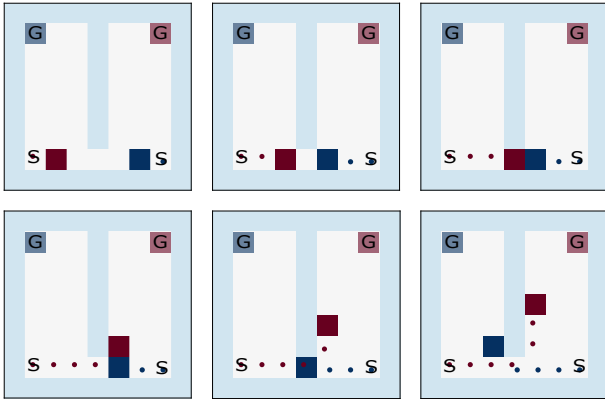


Fig. 16: Two agents trying to reach their respective goal. A narrow passage does not allow simultaneous crossing. Therefore, since each agent sees the other as an obstacle, one of the agents waits for the passage to open, i.e. for a feasible solution to become available.

Then, we have extended the model to account for multiple agents: the agents' Markov models are run in parallel and, in our first approach to the problem, each agent sees the others as moving obstacles (or goals). The emerging behaviors are very realistic and we believe that the consequences of this powerful framework are yet to be explored.

More work is in progress on the following: 1. Application of this framework to real scenes; 2. Inclusion of learning; 3. Inclusion of dynamic rewards; 4. Partial knowledge of goals and obstacles; 5. Partially observable states.

## REFERENCES

- [1] H. Attias, "Planning by probabilistic inference," in *Proc. of the 9th Int. Workshop on Artificial Intelligence and Statistics*, 2003.
- [2] A. Rudenko, L. Palmieri, M. Herman, K. M. Kitani, D. M. Gavrilu, and K. O. Arras, "Human motion trajectory prediction: A survey," *arXiv:1905.06113*, 2019.
- [3] P. Coscia, P. Braca, L. M. Millefiori, F. A. N. Palmieri, and P. Willett, "Unsupervised maritime traffic graph learning with mean-reverting stochastic processes," in *Proceedings of the 2018 21st International Conference on Information Fusion (FUSION 2018)*, 2018.
- [4] P. Coscia, P. Braca, L. M. Millefiori, F. A. N. Palmieri, and P. K. Willett, "Multiple ornstein-uhlenbeck processes for maritime traffic graph representation," *IEEE Transactions on Aerospace and Electronic Systems*, vol. 54, pp. 2158–2170, 2018.
- [5] P. Coscia, L. Ballan, F. Palmieri, A. Alahi, and S. Savarese, *Linear Artificial Forces for Human Dynamics in Complex Contexts*, 2019, vol. 151.
- [6] P. Coscia, F. Castaldo, F. A. N. Palmieri, A. Alahi, S. Savarese, and L. Ballan, "Long-term path prediction in urban scenarios using circular distributions," *Image and Vision Computing*, vol. 69, pp. 81–91, 2018.
- [7] P. Coscia, F. Castaldo, F. A. N. Palmieri, L. Ballan, A. Alahi, and S. Savarese, "Point-based path prediction from polar histograms," in *Proceedings of the 19th International Conference on Information Fusion (FUSION 2016)*, 2016, pp. 1961–1967.
- [8] F. Castaldo, F. Palmieri, and C. Regazzoni, *Application of Bayesian Techniques to Behavior Analysis in Maritime Environments*, 2014, vol. 37.
- [9] C. L. Buckley, C. S. Kim, S. McGregor, and A. K. Seth, "The free energy principle for action and perception: a mathematica review," *Journal of Mathematica Psychologia*, vol. 81, pp. 55–79, 2017.
- [10] T. Parr and K. J. Friston, "Generalised free energy and active inference: can the future cause the past?" *BioARXIV*, 2018.
- [11] M. Baltieri and C. L. Buckley, "An active inference implementation of phototaxis," *ARXIV*, 2017.
- [12] A. Zenon, S. Oleg, and G. Pezzulo, "An information-theoretic perspective on the costs of cognition," *Neuropsychologia*.
- [13] "The anatomy of inference: Generative models and brain structure," *Frontiers in Computational Neuroscience*, 2018.
- [14] R. Kaplan and K. J. Friston, "Planning and navigation as active inference," *Biological Cybernetics*, vol. 112, pp. 323–347, 2018.
- [15] S. Nair, Y. Zhu, S. Savarese, and F.-F. Li, "Causal induction from visual observations for goal directed tasks," *arXiv:1910.01751v1 [cs.LG]* 3 Oct 2019, 2019.
- [16] M. Toussaint and A. Storkey, "Probabilistic inference for solving discrete and continuous state markov decision processes," in *ICML '06 Proceedings of the 23rd international conference on Machine learning*, 2006.
- [17] M. Toussaint, "Probabilistic inference as a model of planned behavior," *Kunstliche Intelligenz*, 2009.
- [18] S. Levine, "Reinforcement learning and control as probabilistic inference: Tutorial and review," *arXiv:1805.00909v3 [cs.LG]* 20 May 2018, 2018.
- [19] (2015) Tensorflow: Large-scale machine learning on heterogeneous systems. [Online]. Available: <https://www.tensorflow.org/>
- [20] F. A. N. Palmieri, "A comparison of algorithms for learning hidden variables in bayesian factor graphs in reduced normal form," *IEEE Transactions on Neural Networks and Learning Systems*, vol. 27, no. 11, pp. 2242–2255, Nov 2016.
- [21] H. A. Loeliger, "An introduction to factor graphs," *IEEE Signal Processing Magazine*, vol. 21, no. 1, pp. 28 – 41, jan. 2004.
- [22] F. Castaldo and F. Palmieri, "Target tracking using factor graphs and multi-camera systems," *IEEE Transactions on Aerospace and Electronic Systems (TAES)*, vol. 51, no. 3, pp. 1950 – 1960, 2015.
- [23] H.-A. . Loeliger, J. Dauwels, J. Hu, S. Korl, P. Li, and F. Kschischang, "The factor graph approach to model-based signal processing," *Proceedings of the IEEE*, vol. 95, no. 6, pp. 1295 –1322, june 2007.
- [24] D. P. Bertsekas, *Reinforcement Learning and Optimal Control*, A. Scientific, Ed., 2019.
- [25] M. L. Puterman, *Markov Decision Processes: Discrete Stochastic Dynamic Programming*, Wiley, Ed., 2005.
- [26] U. B. Kjaerulff and A. L. Madsen, *Bayesian Networks and Influence Diagrams: A Guide to Construction and Analysis*, 2nd ed., S. Nature, Ed., 2012.

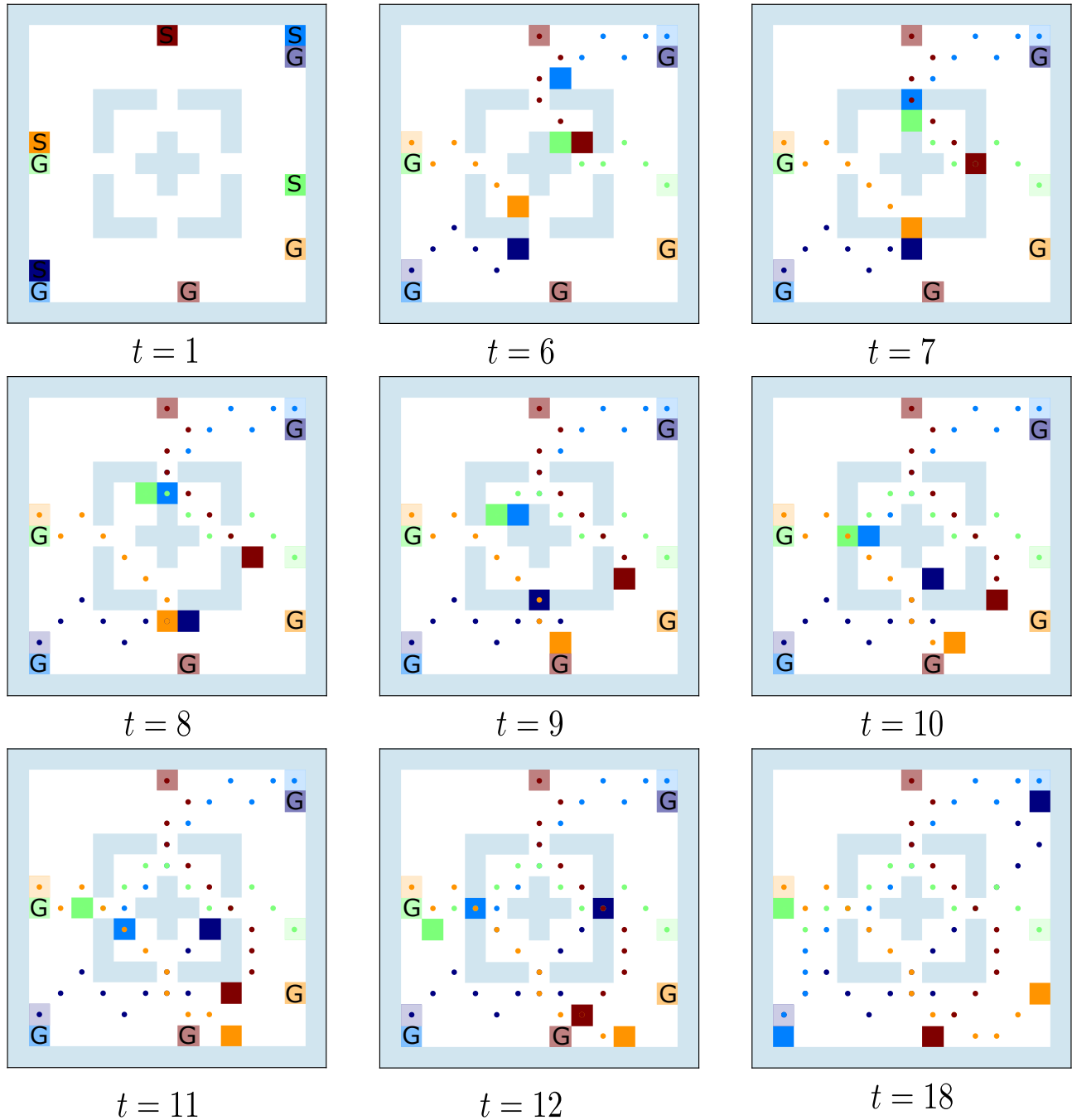


Fig. 17: Five agents try to reach their respective goals (agents and goals are color coded: very light for the start and light for the goal). The picture shows 9 frames ( $t = 1, 6, 7, 8, 9, 10, 11, 12, 18$ ) of a rather complex behavior, where agents may have to cross narrow openings and avoid each other by waiting, changing paths, etc. Various behaviors are worth to note: (a) In frames  $t = 7, 8, 9$ , we can note a conflict between the dark-blue and the orange agents. The orange agent at  $t = 7$  is blocking the passage and the dark-blue agent chooses to go right at  $t = 8$  beginning a new feasible path. However, as soon as the passage opens, the dark-blue agent decides to go back at  $t = 9$ , because that path is better than the one he had initiated. (b) In frame  $t = 7$ , because of the blockage caused by the orange agent, the red agent decides to take an external path, rather than go trough the obstacles. (c) In frame  $t = 10$ , the green agent obstructs the passage for the blue agent that chooses first to go below at  $t = 11$ . Then as soon as the passage opens, he goes back toward that passage at  $t = 12$ , because it corresponds to a better path.